Vol 13 No 7, July 2004
1009-1963/2004/13(07)/1052-07

Chinese Physics

© 2004 Chin. Phys. Soc.
and IOP Publishing Ltd

Polarization-maintaining photonic crystal fibre*

Lou Shu-Qin(娄淑琴)†, Wang Zhi(王 智),
Ren Guo-Bin(任国斌), and Jian Shui-Sheng(简水生)

Institute of Lightwave Technology, Beijing Jiaotong University, Beijing 100044, *China*

(Received 4 September 2003; revised manuscript received 1 March 2004)

Photonic crystal fibres (PCFs) offer new possibilities of realizing highly birefringent fibres due to a higher intrinsic index contrast compared to conventional fibres. In this paper, we analyse theoretically the modal properties of a kind of polarization-maintaining PCF, namely the elliptical hole photonic crystal fibre (EHPCF) with a central small elliptical hole introduced in the core region. We demonstrate the possibility of achieving large birefringence with zero walk-off in the single-mode regime. This PCF also exhibits unusual dispersion properties. Several hundred nanometres of ultra broadband flattened dispersion near the wavelength 1.55μm is achieved in this EHPCF with a central small hole of d_c=0.4Λ.

Keywords: photonic crystal fibre (PCF), birefringence, walk-off parameter, dispersion
PACC: 4281, 4281D, 4281F

1. Introduction

In 1996 a first working example of the so-called 'endlessly single mode photonic crystal fibre' was reported.[1] Since then, intensive research has been promoted by the development of photonic crystal fibres (PCFs). PCFs exhibit many unusual properties such as an endlessly single mode,[1] highly tunable dispersion,[2] and highly controllable mode effective areas for linear and nonlinear applications [3] and so on. However, in all previous works on PCFs it was assumed that the cladding holes are ideally circular-symmetric so that the fundamental mode for such PCFs consists actually of two degenerate modes. This polarization degeneracy may be removed by imperfections of shapes and positions of holes occurring in the processing. Therefore, the polarization state of the output is unpredictable. However, there is a new possibility to create high birefringence in PCFs because its index contrast is higher than with conventional fibres and the stack-and-draw process allows the formation of the required asymmetric microstructure.

Generally, the required birefringence can be achieved in two main ways. The shape of the refractive index profile defining the waveguide can be made non-circular or the material forming the fibre can itself be made birefringent, typically by introducing stresses as in Bow-Tie or Panda fibre. Recently, some highly birefringent PCFs have appeared.[4−6] Among them, elliptical-hole PCF (EHPCF) with elliptical holes instead of the circular holes introduced into its cladding, gives a higher birefringence.[7,8] However, if a small hole is introduced into the core region of the EHPCF,[9] the change gives rise to strong birefringence, and results in a photonic crystal polarization-maintaining fibre with extremely small beat length. So far, there has been no detailed report about the modal properties of an EHPCF with a small central elliptical hole in the core.

In this paper, we analyse the modal properties of EHPCF with a small central elliptical hole in the core using a full-vector model. We have shown that a number of important properties, including the birefringence, walk-off parameter and dispersion are affected. Furthermore, we focus on discussing the dependence of the modal properties on the hole parameter in the core region.

2. The model

The general form of our fibre is indicated in Fig.1. A small elliptical hole is introduced in the centre of the core region. The refractive index of the silica region is

*Project supported by the National High Technology Development Program of China (Grant No 2002AA312190) and the Pandeng Fund of Beijing Jiaotong University (Grant No PD221).
†E-mail: loushuqin@sina.com

1.45. The cladding holes are characterized by the area A' and elliptical ratio $\eta = d/a$, where d and a are the lengths of the major and minor axes. The elliptical ratio of the central small elliptical hole, whose major axis along the y direction is characterized by d_c, is the same as that of elliptical holes in the cladding. Except when we include material dispersion, we express the results in terms of the dimensionless area $A = A'/\Lambda^2$ and frequency $\nu = \Lambda/\lambda$.

To model the polarization properties of the fibre in Fig.1, the scalar approximation becomes inadequate. Here we must use a full vector model of light propagation to accurately predict sensitive properties such as birefringence, walk-off parameter and dispersion.

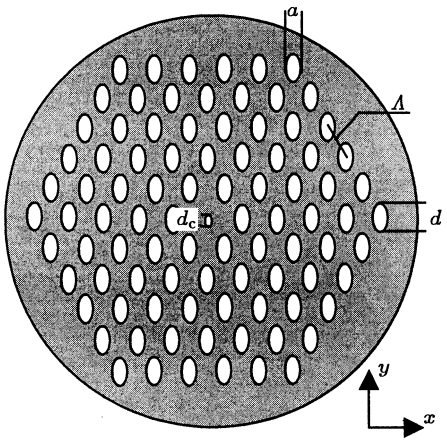


Fig.1. Schematic diagram of the transversal cross section of EHPCF with a central small hole.

Assuming the PCF to be lossless and uniform in the propagation (z) direction, we focus on investigating the transverse mode field distribution, $e_x(x,y)$ and $e_y(x,y)$, which satisfy a pair of coupled wave equations:[10]

$$(\nabla_t^2 - \beta^2 + k^2 n^2) e_x = -\frac{\partial}{\partial x}\left(e_x \frac{\partial \ln n^2}{\partial x} + e_y \frac{\partial \ln n^2}{\partial y}\right),$$
$$(\nabla_t^2 - \beta^2 + k^2 n^2) e_y = -\frac{\partial}{\partial y}\left(e_x \frac{\partial \ln n^2}{\partial x} + e_y \frac{\partial \ln n^2}{\partial y}\right), \quad (1)$$

where $k = 2\pi/\lambda$ is the wavenumber, $n = n(x,y)$ is the transverse refractive index profile, and β is the propagation constant of the corresponding mode.

To solve the above wave equations, we decompose both the transverse refractive index profile and the modal field. The way in which these decompositions are performed is crucial in determining the efficiency and accuracy of the technique.

2.1. Decomposition

2.1.1. Modal field

To solve the coupled wave equations for e_x and e_y, the modal electric field is expanded as

$$e_x(x,y) = \sum_{a,b=0}^{F-1} \varepsilon_{ab}^x \psi_a(x)\psi_b(y),$$
$$e_y(x,y) = \sum_{a,b=0}^{F-1} \varepsilon_{ab}^y \psi_a(x)\psi_b(y), \quad (2)$$

where F is the number of terms retained in this expansion, $\psi_i(s)$ $(i = a, b,\ s = x, y)$ are elements of the orthogonal set of Hermite–Gaussian basis functions:

$$\psi_i(s) = \frac{2^{-i/2}\pi^{-1/4}}{\sqrt{(i)!\omega}} \exp\left(-\frac{s^2}{2\omega^2}\right) H_i(s/\omega), \quad (3)$$

where H_i (s/ω) is the ith-order Hermite polynomial, ω is the characteristic width of the basis set.

2.1.2. Transverse refractive index profile

The supercell lattice method [11] is used to describe the transverse dielectric structure of PCF, and two 2D virtual perfect photonic crystals (PC1 and PC2) are introduced. The periodic lattice of holes is described by periodic functions (cosines). The dielectric structure of the supercell lattice can be reconstructed as the decomposition of PC1 and PC2. The way in which the decomposition is achieved is sketched

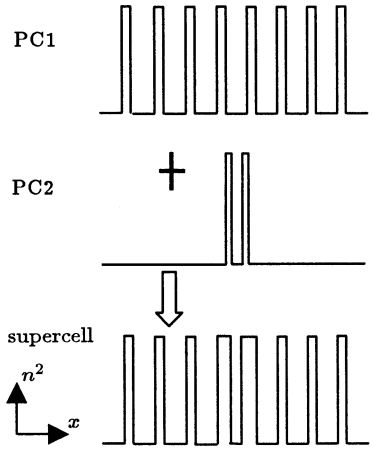


Fig.2. Schematic of the way in which the transverse refractive index profile is decomposed. Here a cross section along the x-axis is shown.

in Fig.2. The dielectric constant of the PCF can be expressed as the sum of the decomposition of PC1 and PC2:

$$n^2(x,y) = \sum_{a,b=0}^{P_1-1} P_{1ab} \cos\frac{2\pi a x}{l_{1x}} \cos\frac{2\pi b y}{l_{1y}} + \sum_{a,b=0}^{P_2-1} P_{2ab} \cos\frac{2\pi a x}{l_{2x}} \cos\frac{2\pi b y}{l_{2y}}, \quad (4a)$$

$$\ln n^2(x,y) = \sum_{a,b=0}^{P_1-1} P_{1ab}^{\ln} \cos\frac{2\pi ax}{l_{1x}} \cos\frac{2\pi by}{l_{1y}} + \sum_{a,b=0}^{P_2-1} P_{2ab}^{\ln} \cos\frac{2\pi ax}{l_{2x}} \cos\frac{2\pi by}{l_{2y}}, \quad (4b)$$

where P_1 and P_2 are the numbers of decomposition terms of PC1 and PC2, respectively, l_{1x}, l_{1y}, l_{2x} and l_{2y} are the characteristic lengths along the x or y axis of PC1 and PC2, P_{1ab}, P_{2ab}; $P_{1ab}^{\ln}$ and $P_{2ab}^{\ln}$ are the decomposition coefficients which can be obtained through the Fourier transform [11] of the periodic dielectric structures for both PC1 and PC2. By choosing the corresponding decomposing parameter, the index can be reproduced accurately and efficiently. Note that we decompose the squared refractive index n^2, rather than n. This leads to much simpler forms of the overlap integrals, shown below.

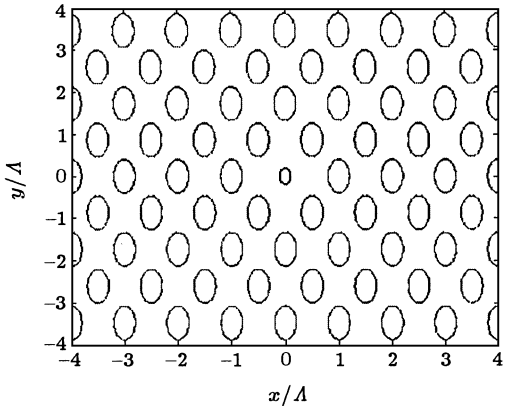


Fig.3. The refractive index reconstruction when P_1=100 and P_2=500 for a fibre with d/Λ=0.8, d_c/Λ=0.4 and η=2.

Figure 3 demonstrates how well our decomposition method can reproduce the complicated transverse index structure in a holey fibre. It shows the reconstruction of the index profile for a fibre with d/Λ=0.8, d_c/Λ=0.4 and η=2 (as defined in Fig.1) when the decomposition term P_1=100 and P_2=500. Figure 4 shows a cross section reconstructed through this profile along the y=0 axis. Figures 3 and 4 show that the index can be reproduced quite accurately with periodic functions (cosines).

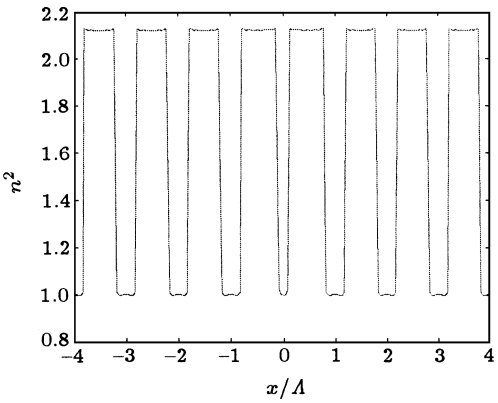


Fig.4. Cross sections along the y=0 axis of the index reconstruction for a fibre with d/Λ=0.8, d_c/Λ=0.4 and η=2 when P_1=100 and P_2=500.

2.2. Eigenvalue system

With the decomposition method described in Sec.2.1, the vector wave equation is then reduced to the following eigenvalue systems:

$$L\begin{bmatrix}\varepsilon^x\\ \varepsilon^y\end{bmatrix} \equiv \begin{bmatrix} I_{abcd}^{(1)} + k^2 I_{abcd}^{(2)} + I_{abcd}^{(3)x} & I_{abcd}^{(4)x} \\ I_{abcd}^{(4)y} & I_{abcd}^{(1)} + k^2 I_{abcd}^{(2)} + I_{abcd}^{(3)y} \end{bmatrix} \begin{bmatrix}\varepsilon^x\\ \varepsilon^y\end{bmatrix} = \beta_j^2 \begin{bmatrix}\varepsilon^x\\ \varepsilon^y\end{bmatrix}, \quad (5)$$

where β_j is the propagation constant of the corresponding transverse mode (e_x, e_y), $I^{(1)}$,$I^{(2)}$, $I^{(3)}$ and $I^{(4)}$ are overlap integrals of the modal functions, which have been defined in our previous work.[11]

Substituting the decomposition equation (4) into Eq.(5), the overlap integrals can be calculated using the orthonormality of the Hermite–Gaussian basis functions and the standard integration-by-parts technique combined with some of the definite integrals available in collections along with some identities.[12] It is a significant advantage that all these integrals can be obtained analytically, and the numerical precision and efficiency can be improved greatly, especially when a large number of terms are used in the expansions. When evaluated, the expressions for these overlap integrals become quite complicated, and they are not given here; the analogous expressions can be found in Refs.[11,13].

By solving Eq.(5) at a particular wavelength λ, the modes and the corresponding β_j of the PCF at λ can be calculated. As L is a $(2\times F^2)\times(2\times F^2)$ matrix, the eigenvalue problem can be solved to produce $2\times F^2$ eigenvalues and their corresponding eigenvectors. Only a few of the eigenvalue–eigenvector pairs are physically relevant quantities corresponding to the guided modes of the fibre. The other eigenvalues are related to radiation modes of the fibre. The transverse modal electric field can be obtained by substituting

the eigenvector into the decomposition equation (2).

3. Polarization properties

3.1. Birefringence

Presumably, the parameter of the greatest interest is the birefringence of the fundamental mode, which is defined as the effective index difference between the y-polarized mode and the x-polarized modes, i.e. $B = \Delta n_{\text{eff}} = |n_{\text{eff}}^{y} - n_{\text{eff}}^{x}|$. The effects of the area of elliptical holes and the elliptical ratio in the cladding on birefringence are similar to those of EHPCF, which had been discussed in Ref.[7]. Here we concentrate on the effect of the small central hole in the core region on birefringence.

The effect of the small central hole on birefringence is shown in Fig.5 for a fibre with elliptical ratio η=3, hole areas A=0.3 (solid line) and A=0.1 (dashed line). The birefringence increases monotonically with the increase in the size of the small hole. For instance, at the frequency ν=1.3 and hole area A=0.3, the birefringence has 2.121×10^{-3} for EHPCF without the central hole (d_c=0). If the central hole changes to d_c=0.6d, birefringence attains 8×10^{-3}. Therefore, the EHPCF with a small central hole has a much higher birefringence than without it. Furthermore, the larger the elliptical holes in the cladding, the more notable the effect of the small central elliptical hole on birefringence, especially in the middle region of the frequency shown in Fig.5.

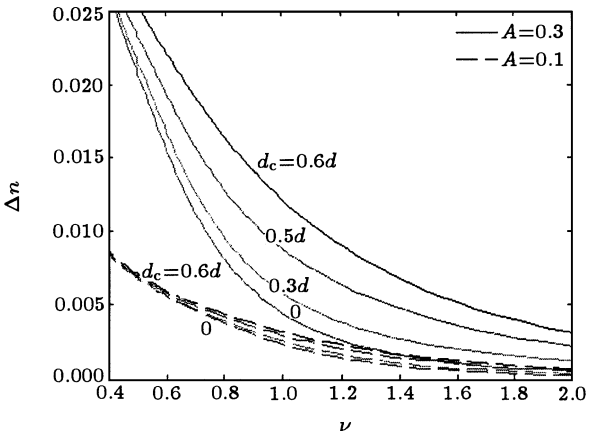


Fig.5. Birefringence Δn for A=0.3 (solid line) and A=0.1 (dashed line). For each hole area A in the cladding, curves are shown for different central holes d_c=0, 0.3d, 0.5d, 0.6d, birefringence increasing with the central hole increasing.

Recalling the behaviour of conventional polarization maintaining fibres,[14] their birefringence tends to zero at both high and low frequencies. At high frequencies, the vector terms in the wave equation become negligible, while at low frequencies, the bulk of the mode energy is distributed far from the core-cladding interface. These lead to reduction of the birefringence. The birefringence of the EHPCF with a small central hole in Fig.5 shows very different behaviour. It is typically stronger than the conventional fibres for comparable parameters. While it must vanish in the scalar regime at high frequencies, the long wavelength response changes to a monotonic increase with decreasing frequency. The long wavelength behaviour is due to the cladding region, which acts as a birefringence material. The birefringence increases with hole areas, as might be expected, since the larger holes represent a stronger perturbation to the field.

On the other hand, the field penetrates even further into the periodic cladding region in the long regime. More and more mode energy is located beyond the first ring of air holes. Therefore, the field tends to approach the distribution of the FSM state as closely as possible.[7] It thus can be concluded that the birefringence between the mode FSMy and FSMx must be the maximum value at a fixed wavelength for a PCF.

At a fixed d/Λ and λ/Λ, as the central small hole diameter d_c/Λ increases from 0, Δn increases. Once the central small hole increases to the same size as the cladding holes, the PCF becomes a perfect photonic crystal, hence the fundamental mode is the FSM mode. Therefore, Δn should reach its peak at the point $d_c/\Lambda \cong d/\Lambda$. Fortunately, this conclusion is verified by the numerical results as shown in Fig.6 where the cladding hole size is d/Λ=0.7. Δn increases with increasing d_c/Λ. When d_c/Λ is close to 0.7, Δn reaches its peak and then decreases.

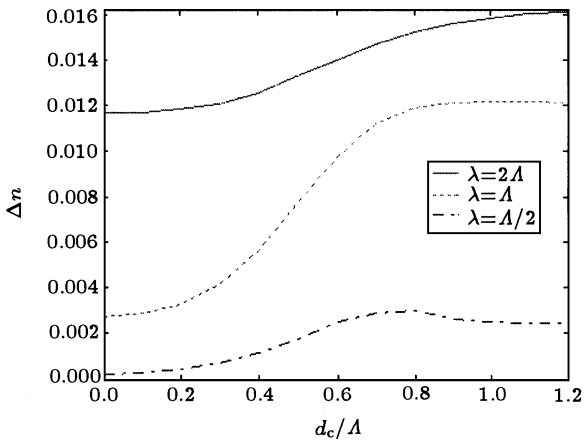


Fig.6. Δn versus d_c/Λ at different wavelengths.

In a word, the presence of a small central hole in the core gives rise to larger birefringence than in the case without the hole. If there is an increase in the size of the central hole, or in the elliptical hole areas in the cladding, birefringence for the EHPCF will increase. This result offers a new way to design high performance polarization maintaining fibres through choosing the size of a small central elliptical hole, or the elliptical hole areas in the cladding.

3.2. Group index and walk-off parameter

For pulsed propagation in birefringent systems, the walk-off parameter, defined as

$$\Delta n_{\rm g} = n_{\rm g}^{y} - n_{\rm g}^{x}, \tag{6}$$

is as important as the birefringence itself. It determines the rate at which orthogonally polarized pulses separate on propagation. In fact, $\Delta n_{\rm g}$ is the first-order polarized mode dispersion (PMD). Usually we calculate the group indices $n_{\rm g}^{y}$ and $n_{\rm g}^{x}$ of two orthogonally polarized pulses as

$$n_{\rm g} = c\frac{{\rm d}\beta}{{\rm d}\omega} = n_{\rm eff} + \nu\frac{{\rm d}n_{\rm eff}}{{\rm d}\nu}. \tag{7}$$

The walk-off parameter may then be expressed as

$$\Delta n_{\rm g} = \Delta n_{\rm eff} + \nu\frac{{\rm d}\Delta n_{\rm eff}}{{\rm d}\nu}. \tag{8}$$

Figure 7 shows $\Delta n_{\rm g}$ as a function of frequency ν for different sizes of central hole for η=3, A=0.1 (dashed line) and A=0.3 (solid line).

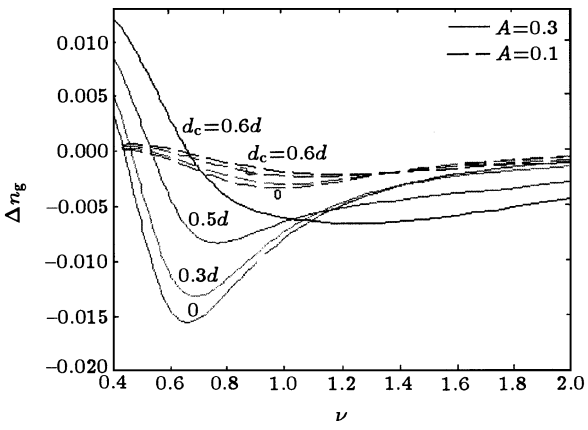


Fig.7. Walk-off parameter $\Delta n_{\rm g}$ for A=0.3 (solid line) and A=0.1 (dashed line). For each hole area A in the cladding, curves are shown for different central holes $d_{\rm c}$=0, 0.3d, 0.5d, 0.6d, walk-off increasing with the central hole increasing.

The walk-off parameter of EHPCF with a central hole increases quickly as the size of the central hole increases. The magnitude of the walk-off parameter for these fibres is larger than that of EHPCF without the central hole ($d_{\rm c}$=0), as shown in Fig.7.

The characteristics of walk-off parameter for this fibre are different from those of the conventional PMF.[14] In keeping with the strong birefringence in Fig.5, the magnitude of walk-off is again larger than that for the conventional PMF. More importantly, the zero-crossing and negative walk-off region occurs at much longer wavelengths than for conventional PMF. Moreover, the zero walk-off point appears well inside the single-mode regime.[9] This downward shift of the zero walk-off point is associated with the nonzero value of the long wavelength birefringence that we have described in Fig.5. Since the low frequency limit of $n_{\rm eff}^{x}$ is lower than $n_{\rm eff}^{y}$, $\Delta n_{\rm eff} = n_{\rm eff}^{y} - n_{\rm eff}^{x}$ is greater than zero. The quantity ${\rm d}n_{\rm eff}/{\rm d}\nu < 0$ for all ν is shown in Fig.5. Thus the second term in (8) pushes the walk-off to negative values more quickly than for standard fibres. Combined with the suppression of higher order modes in the PCF, we obtain the effect of zero walk-off in a single-mode regime—these fibres can be constructed to produce a vanishing first-order PMD at a given wavelength.

The walk-off parameter increases as the size of the central hole increases and the zero walk-off point shifts slightly towards the high frequency regime. Comparing the walk-off curve with the same small central hole and different cladding hole A=0.1 and A=0.3, the walk-off parameter increases with an increase in the hole area of the cladding and the zero walk-off point shifts toward the low frequency regime. It is seen from Fig.7 that the magnitude of positive walk-off increases distinctly with decreasing frequency at the low frequency regime. However, the increase in walk-off as $\nu \to 0$ does not continue indefinitely. Recall that the FSM dispersion curve flattens out at long wavelength [7] and that the bound modes approach the FSM curves in that regime. Therefore, both birefringence and walk-off parameter must also become constant at very long wavelengths with $\Delta n_{\rm FSM} = \Delta n_{\rm eff} = \Delta n_{\rm g}$. This can be ascertained from the behaviour of the corresponding walk-off parameter curve with A=0.1 in the low frequency regime.

For the EHPCF with a small central hole in the core, we can get zero walk-off point in the low frequency regime that is located in the single mode regime by adjusting the size of the hole, or the area of the cladding elliptical holes. This conclusion is very important for the design of fibres suitable for actual

application. We can design PCFs that operate in a single mode with zero walk-off and high birefringence at a given wavelength, or that operate at a single polarized mode with high birefringence and large walk-off. It is difficult to get such characteristics in conventional fibres.

4. Dispersion

The total dispersion coefficient D_t is proportional to the second order derivative of the modal effective index (or the propagation constant) with respect to the wavelength λ. Generally, the total dispersion coefficient D_t should be expressed as the sum of the waveguide dispersion D_w and the material dispersion D_m, and D_m can be calculated by applying the Sellmeyer law. Because PCF is made of silica, the material dispersion is the same for PCFs with different structure parameters; the waveguide dispersion D_w is a crucial factor for calculating the total dispersion coefficient. The waveguide dispersion is expressed as

$$D = \frac{d\tau}{d\lambda} = -\frac{\lambda}{c}\frac{d^2 n_{eff}}{d\lambda^2}. \quad (9)$$

Considerable attention has been devoted to the ability of photonic crystal fibres to generate novel group velocity dispersion profiles. In Fig.8, we illustrate EHPCF with a small central hole in the core to demonstrate some of these ideas. We show dispersion profiles for x- and y-polarized modes for four fibres with different central holes; the relative hole diameter d/Λ=0.8 in the cladding and elliptical ratio η=3.

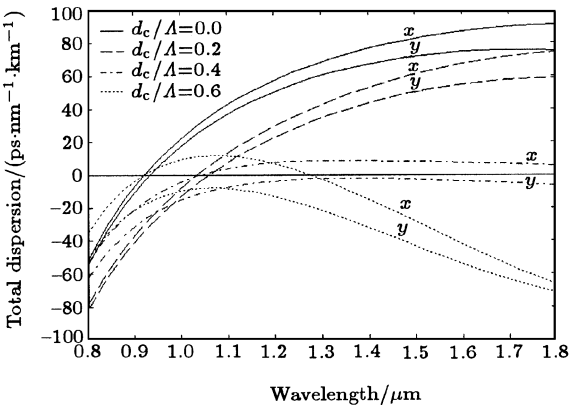


Fig.8. Dispersion of two fundamental modes, x-polarized mode and y-polarized mode, for EHPCF with different central small holes in the core region, d/Λ=0.8 and η=3.

Due to the elliptical shape of the holes in these fibres, the polarization degeneracy of the fundamental mode is removed. The dispersion curves of x-polarized mode and y-polarized mode separate from each other. The x-polarized mode is located above the y-polarized mode. Its dispersion rises faster than that of the y-polarized mode. The dispersion relation rises faster when the central hole has a small value: for example, d_c/Λ=0 as shown in Fig.8. Then the rising speed becomes slightly slower with an increase in the size of the hole. When d_c/Λ=0.4, the dispersion curve flattens and we get a flat profile over several hundreds of nanometres around λ=1.55μm in which the two modes show dispersion of 8ps/nm·km and -3ps/nm·km. When the central small hole continues growing, the profiles are no longer flat and the dispersion become negative in the long wavelength regime and we obtain two zero dispersion points at d_c/Λ=0.6 d/Λ, one near λ=935nm and another near λ=1300nm. There is clearly scope for considerable design exploration.

5. Discussion and conclusion

The full vector supercell overlapping method, based on our previous work, is an effective predictive tool allowing us to calculate the modal properties of a much fuller range of holey fibres than scalar techniques. It is an efficient and accurate alternative to existing techniques. This method has been used for analysing the triangular PCF.[11,13] The results accord with the result of other numerical methods [14–20] and experiment.[1]

Here we have shown that the complicated structure of EHPCF with a central smaller elliptical hole leads to highly unusual and tailorable modal properties. For example, in Sec.3.1, we showed that birefringence in this EHPCF is larger than that of EHPCF with out the central hole, and in Sec.3.2 we obtained unusual walk-off properties such as zero walk-off point at low frequency and single mode regime, and zero walk-off with high birefringence at a given wavelength. This feature can be used for the design of some special fibres that can be operated at zero walk-off and single mode regime at a given wavelength. This can efficiently restrain first order PMD. In Sec.4, we obtained a flat profile over several hundred nanometres around λ=1.55μm at d_c/Λ=0.4 and also obtained two zero dispersion points at d_c/Λ=0.6. This feature can be used for the design of ultra-low dispersion and ultra-flat dispersion PCFs.

In conclusion, the EHPCF with a central small elliptical hole offers the possibility of obtaining these unusual properties through choice of a suitable size of

the central hole, or of the hole areas in the cladding. In other words, the EHPCF with a central small elliptical hole has a high degree of flexibility, and can be designed to suit a very wide range of applications. Moreover, the method we have developed here can also be used to analyse other kinds of PCF.

References

[1] Birks T A, Knight J C and Russell P St J 1997 *Opt. Lett.* **22** 961

[2] Kunimasa Saitoh and Masanori Koshiba 2002 *IEEE Photon. Technol. Lett.* **14** 1291

[3] Wadsworth W J and Knight J C 2000 *Electron. Lett.* **36** 53

[4] Ortigosa–Blanch A, Knight J C, Wadsworth W J *et al* 2000 *Opt. Lett.* **25** 1325

[5] Suzuki K, Kubota H, Kawanishi S *et al* 2001 *Electron. Lett.* **37** 1399

[6] Kunimasa Saitoh and Masanori Koshiba 2002 *IEEE Photon. Technol. Lett.* **14** 1291

[7] Steel M J and Osgood P M 2001 *J. Lightwave Technol.* **19** 495

[8] Ren G B, Wang Z, Lou S Q *et al* 2004 *Acta Phys. Sin.* **53** 484 (in Chinese)

[9] Jes Brong, Dmitri Mogilevtsev, Stig E *et al* 2001 *Laser and Electro-Optics, CLEO/Pacific Rim* I6

[10] Snyder A W and Love J D 1985 *Optical Waveguide Theory* (London: Chapman and Hall)

[11] Ren G B, Wang Z, Lou S Q *et al* 2003 *Opt. Express* **11** 1310

[12] Gradshtein I S and Ryzhik I M 1994 *Tables of Integrals, Series and Products* (New York: Academic)

[13] Wang Z, Ren G B, Lou S Q *et al* 2003 *Opt. Express* **11** 980

[14] Dyott R B 1995 *Elliptical Fiber Waveguides* (Boston, MA: Artech House)

[15] Monro T M, Richardson D J, Broderick N G R *et al* 2000 *J. Lightwave Technol.* **18** 50

[16] Monro T M, Richardson D J and Broderick N G R 1999 *Optical Fiber Communication Conference* **FG3** 111

[17] Mogilevtsev D, Birks T A and Russell P St 1999 *J. Lightwave Technol.* **17** 2078

[18] Koshiba M 2002 *IEICE Electron.* **4** 881

[19] Li S G, Liu X D and Hou L T 2004 *Acta Phys. Sin.* **53** 1873 (in Chinese)
Li S G, Liu X D and Hou L T 2004 *Acta Phys. Sin.* **53** 1880 (in Chinese)

[20] Wang M G, Li T J and Jian S S 2003 *Acta Phys. Sin.* **52** 609 (in Chinese)